Gold Cyanidation Behavior of Limonitic Ores from the Carajás Province, Brazil: Mineralogical Controls, Cyanide Consumption, and Leaching Kinetics.

Antonio Clareti Pereira

PhD in Chemical Engineering São Paulo University – USP Belo Horizonte – MG – Brazil

DOI: https://doi.org/10.47772/IJRISS.2026.100600467

Received: 10 June 2026; Accepted: 15 June 2026; Published: 26 June 2026

ABSTRACT

Limonitic gold ores constitute an important resource for global gold production; however, their mineralogical heterogeneity and the occurrence of cyanide-consuming phases may significantly influence metallurgical performance and operating costs. This study investigates the cyanidation behavior of gold-bearing limonitic ores from the Carajás Mineral Province, northern Brazil, with emphasis on the relationships between mineralogical composition, gold extraction, cyanide consumption, and sulfur content. Four representative drill-core samples underwent detailed chemical and mineralogical characterization using ICP-OES, SEM-EDS, and QEMSCAN, followed by dynamic and kinetic cyanidation tests. An additional ten samples from the same limonitic weathering domain were evaluated through standardized 8 h cyanidation tests to validate the metallurgical response of the ore population.

The investigated ores contained between 14 and 77 wt.% iron oxyhydroxides, confirming variable degrees of lateritic weathering, while copper concentrations ranged from 0.02 to 0.30 wt.%. Dynamic cyanidation tests performed on material ground below 75 μm achieved average gold recoveries of approximately 89–90%, indicating predominantly free-milling behavior. Kinetic leaching experiments demonstrated rapid gold dissolution, with approximately 90% of the final recovery achieved within 8 h of cyanidation, corresponding to an average sodium cyanide consumption of approximately 650 g NaCN/t ROM. Mineralogical observations revealed that copper-bearing phases were the primary contributors to cyanide consumption, whereas iron oxyhydroxides had little effect on gold extraction efficiency.

The expanded dataset comprising fourteen samples confirmed the favorable cyanidation characteristics of the limonitic ores, with most samples exhibiting gold recoveries above 90%. Statistical analysis further indicated a strong inverse relationship between sulfur content and gold recovery, suggesting that residual sulfide mineralization may locally reduce cyanidation performance despite the predominantly oxidized nature of the deposit. These findings demonstrate the importance of integrating mineralogical characterization, kinetic leaching studies, and statistical validation to optimize cyanidation performance and support the development of efficient processing routes for oxidized gold deposits.

Keywords: Gold cyanidation; Limonitic ore; Lateritic gold deposit; Gold extraction; Cyanide consumption; Copper minerals; Leaching kinetics; Carajás Province.

Highlights

1. Gold recoveries of approximately 90% were achieved by cyanidation.
2. Limonitic ores contained up to 77 wt.% iron oxyhydroxides.
3. Gold extraction was not significantly affected by iron oxyhydroxides.
4. Copper-bearing minerals were the main cyanide-consuming phases.
5. Approximately 90% gold recovery was obtained after only 8 h of leaching.

Graphical abstract

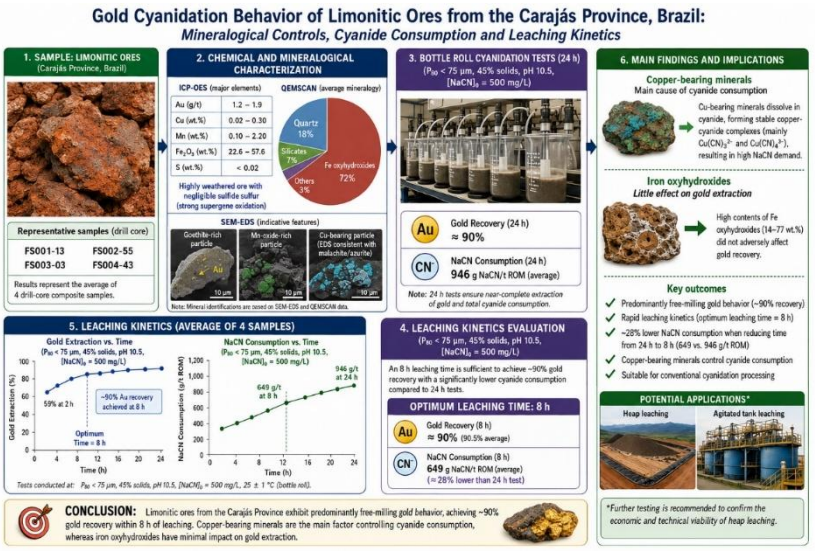

INTRODUCTION

Gold remains one of the most strategically important metals worldwide due to its applications in investment markets, electronics, medicine, and advanced technologies. Despite continuous exploration efforts, the proportion of easily processed high-grade deposits has steadily declined, leading to increased exploitation of low-grade, oxidized, and weathered ores (Nicol, 2022; Sekisov & Rasskazova, 2021). As a result, understanding the factors controlling gold recovery from complex ore types has become increasingly important for the economic and sustainable development of mineral resources.

Limonitic gold ores represent a significant portion of oxidized deposits occurring in tropical and subtropical regions. These ores typically form through intense weathering of primary sulfide mineralization and are characterized by abundant iron oxyhydroxides, including goethite, ferrihydrite, and limonite (Costa et al., 2022; Huang et al., 2025). Compared with refractory sulfide ores, oxidized ores generally exhibit improved gold accessibility to cyanide solutions; however, variations in mineralogical composition, weathering intensity, and the presence of cyanide-consuming phases may strongly influence metallurgical performance and reagent consumption (Asamoah et al., 2021; Chingwaru et al., 2025).

Cyanidation remains the dominant industrial process for gold extraction because of its high efficiency, operational simplicity, and economic viability (Nicol, 2022; Bracamontes-Landavazo et al., 2024). Nevertheless, the performance of cyanidation is highly dependent on ore mineralogy. In oxidized gold ores, cyanide consumption is frequently associated with the presence of copper-bearing minerals, manganese oxides, and other reactive phases capable of consuming cyanide or oxygen during leaching. Copper minerals are particularly important because they form stable copper-cyanide complexes, reducing the concentration of free cyanide available for gold dissolution and increasing operating costs (Pereira et al., 2017; Chen et al., 2020). In addition, iron oxyhydroxides may influence gold recovery through adsorption processes and mineralogical associations with fine gold particles (Huang et al., 2025; Roostaei et al., 2025, 2026).

Recent advances in process mineralogy, automated mineralogical characterization, and diagnostic metallurgical testing have demonstrated the importance of integrating geological, mineralogical, and metallurgical information to predict ore behavior and optimize processing routes (Ofori-Sarpong et al., 2020; Guner et al., 2023; Chen et al., 2025). Such approaches are particularly relevant for weathered gold deposits, where significant heterogeneity may occur over relatively short spatial scales.

The Carajás Mineral Province, located in northern Brazil, hosts extensive lateritic and iron-rich weathering profiles associated with some of the world's largest mineral deposits. Although the geology and iron ore resources of the region have been extensively studied, comparatively little information is available regarding the cyanidation behavior of limonitic gold ores developed within these weathering environments. Understanding the

relationships between mineralogical composition, sulfur content, cyanide consumption, and gold recovery is therefore important for both process optimization and resource evaluation.

The present study investigates the cyanidation behavior of gold-bearing limonitic ores from the Carajás Mineral Province through integrated chemical, mineralogical, and metallurgical characterization. Four representative samples were subjected to detailed ICP-OES, SEM-EDS, and QEMSCAN analyses, followed by dynamic and kinetic cyanidation tests. To assess the variability and representativeness of the metallurgical response, an additional ten samples from the same limonitic weathering domain were evaluated through standardized 8 h cyanidation tests. The study aims to identify the principal mineralogical controls on gold extraction and cyanide consumption, evaluate the influence of sulfur-bearing phases, and establish the metallurgical characteristics of limonitic gold ores from the Carajás region.

LITERATURE REVIEW

Gold Occurrence in Limonitic and Lateritic Ores

Limonitic and lateritic gold ores are formed through prolonged weathering of primary mineral deposits under tropical and subtropical climatic conditions. During lateritization, sulfide minerals are progressively oxidized, producing iron-rich weathering profiles dominated by goethite, hematite, limonite, and ferrihydrite (Costa et al., 2022). These weathering processes commonly improve gold liberation relative to primary sulfide ores, although the resulting mineralogical assemblages may still exert significant control over metallurgical performance.

Gold in oxidized deposits may occur as liberated particles, inclusions within iron oxyhydroxides, grain-boundary precipitates, nanoparticles adsorbed onto iron oxide surfaces, or in association with manganese oxides and clay minerals. Supergene enrichment processes frequently concentrate gold within ferruginous horizons, resulting in heterogeneous gold distributions throughout the weathering profile (Bragin et al., 2019; Huang et al., 2025). Recent studies employing automated mineralogical techniques such as QEMSCAN, MLA, and SEM-EDS have demonstrated that gold occurrence and mineral associations strongly influence cyanide accessibility and extraction efficiency (Chingwaru et al., 2025; Guner et al., 2023).

Cyanidation of Oxidized Gold Ores

Cyanidation remains the dominant industrial technology for gold extraction because of its high efficiency, technological maturity, and economic viability (Nicol, 2022; Bracamontes-Landavazo et al., 2024). Gold dissolution occurs in alkaline cyanide solutions under oxidizing conditions, producing the stable dicyanoaurate complex according to Elsner's reaction:

$$4Au+8CN^{-}+O_2+2H_2O \rightarrow 4[Au(CN)_2]^{-}+4OH^{-}$$

The efficiency of cyanidation depends on several factors, including particle size, mineral liberation, oxygen availability, cyanide concentration, pH, and the occurrence of cyanide-consuming minerals. Compared with refractory sulfide ores, oxidized ores generally exhibit superior cyanidation performance because weathering destroys much of the sulfide matrix that originally encapsulated gold particles. Consequently, many limonitic ores display free-milling behavior and can achieve gold recoveries exceeding 80–90% without intensive pretreatment (Deveci et al., 2023; Sekisov & Rasskazova, 2021). Nevertheless, considerable variability exists among oxidized deposits, particularly where residual sulfides, manganese oxides, or iron oxyhydroxides influence gold accessibility and reagent consumption.

Iron Oxyhydroxides and Mineralogical Controls on Gold Recovery

Iron oxyhydroxides constitute the dominant mineralogical component of many limonitic ores. Goethite, ferrihydrite, and amorphous iron oxides possess high specific surface areas and significant adsorption capacities, making them important phases in weathered gold systems (Pereira et al., 2018; Huang et al., 2025). Several studies have reported that dissolved gold species may interact with iron oxide surfaces via adsorption, although

these effects are generally less severe than the preg-robbing behavior observed in carbonaceous ores (Roostaei et al., 2025).

In addition to adsorption phenomena, iron oxyhydroxides may act as hosts for ultrafine gold particles generated during supergene enrichment. In such cases, gold recovery becomes largely controlled by mineral liberation rather than by leaching chemistry alone (Roostaei et al., 2026). The abundance of iron oxyhydroxides may also influence pulp rheology, oxygen transfer, and reagent distribution during cyanidation. Consequently, detailed mineralogical characterization is essential for understanding the metallurgical response of limonitic gold ores and for identifying the factors controlling gold extraction.

Cyanide Consumption and Gold Leaching Kinetics

Cyanide consumption significantly affects gold cyanidation. Many minerals, especially copper-bearing phases, can reduce free cyanide by dissolving in cyanide solutions and forming stable complexes. Copper minerals like malachite, azurite, chrysocolla, tenorite, and cuprite are primary cyanide consumers in oxidized gold deposits (Pereira et al., 2017; Chen et al., 2020).

Manganese oxides may also contribute to cyanide losses through catalytic oxidation reactions, whereas residual sulfide minerals can increase oxygen demand and reduce cyanidation efficiency. Consequently, the mineralogical composition of the ore strongly influences reagent consumption and operating costs.

Gold dissolution kinetics depend on mineral liberation, particle size, oxygen, cyanide concentration, and mass transfer. Free-milling ores often dissolve quickly at first, then slow down. Finding the optimal leaching time is crucial, as longer leaching times rarely improve recovery but greatly increase reagent use. Combining extraction kinetics, cyanide use, and mineralogy helps optimize performance and conditions for oxidized gold ores.

MATERIALS AND METHODS

Ore Sampling and Preparation

The limonitic gold ores studied were from diamond drill cores in the Carajás Mineral Province, Pará, Brazil. Four samples from different drills and depths (Samples 01- 04) were chosen for mineralogical and metallurgical analysis. Ten more Samples (Samples 05- 04) from the same weathering zone validated the ore's metallurgical response.

Samples were taken from weathered limonitic profiles in the Carajás Mineral Province, a major mineral district with giant iron deposits. Though from different sectors, all samples came from intensely weathered ferruginous terrains with similar geological features. The location and sites are shown in Figure 1.

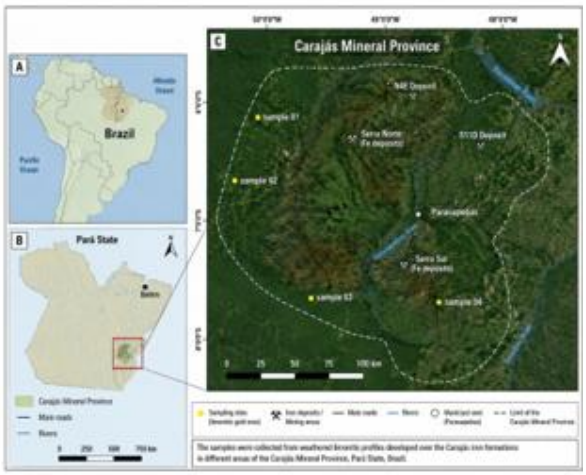

Figure 1. Geographic location of the Carajás Mineral Province and sampling sites investigated in this study. (A) Location of the study area within Brazil; (B) location of the Carajás Mineral Province in Pará

State; and (C) distribution of the limonitic gold ore sampling sites (01, 02, 03 and 04) within the Carajás Mineral Province. Source: Satellite imagery adapted from Google Earth Pro and modified by the authors.

The four representative samples (Samples 01–04) were subjected to detailed chemical characterization, QEMSCAN analysis, SEM-EDS investigation, dynamic cyanidation tests, and kinetic leaching experiments. The additional ten samples (Samples 05–14) were evaluated through standardized 8 h cyanidation tests to assess variability in metallurgical performance and to provide statistical validation of the cyanidation behavior observed in the detailed study samples.

All samples were initially crushed to a top size of 6.35 mm and homogenized. Subsamples of approximately 1 kg were prepared for cyanidation tests. Additional portions were crushed below 1.0 mm, homogenized, and split for chemical and mineralogical characterization. For dynamic cyanidation experiments, representative aliquots were further ground to a particle size of less than 75 μm.

Dynamic cyanidation tests were performed in triplicate, whereas kinetic leaching tests were conducted in duplicate to evaluate experimental reproducibility.

Chemical Characterization

Gold grades were determined by fire assay followed by cupellation and atomic absorption spectrometry (AAS). The analytical detection limit for gold was 0.005 mg/kg.

Major and minor elements were analyzed using inductively coupled plasma optical emission spectrometry (ICP-OES). Sample preparation involved lithium metaborate fusion followed by acid dissolution. The fused samples were dissolved in 10% (v/v) nitric acid with continuous agitation prior to instrumental analysis.

Carbon analyses were performed to quantify inorganic carbon associated with carbonate minerals. Samples were treated with hydrochloric acid, converting carbonates into carbon dioxide, which was subsequently measured using a non-dispersive infrared detector (NDIR).

Mineralogical Characterization

Mineralogical characterization was carried out using Quantitative Evaluation of Minerals by Scanning Electron Microscopy (QEMSCAN) and scanning electron microscopy coupled with energy-dispersive spectroscopy (SEM-EDS) (Stephen et al., 2021).

Polished sections were prepared from each sample and analyzed using a QEMSCAN 650 system equipped with dual Bruker silicon drift detectors (SDD-EDS). Measurements were performed at an accelerating voltage of 25 kV and a beam current of 10 nA under standard operating conditions (Chen et al., 2025).

Mineral identification and modal mineralogy were obtained through automated mineralogical analysis. Particular attention was given to identifying iron oxyhydroxides, quartz, clay minerals, and other phases that may influence cyanide consumption and gold recovery. SEM-EDS investigations were additionally performed to evaluate mineral associations, textural relationships, and the occurrence of potentially cyanide-consuming phases such as copper-bearing minerals, manganese oxides, and iron oxyhydroxides (Guner et al., 2023).

Gold Occurrence and Automated Mineralogical Analysis

The occurrence, morphology, and spatial distribution of gold particles were investigated using automated mineralogical analysis and SEM-EDS observations. Polished sections prepared from Samples 01–04 were examined to identify gold-bearing particles, evaluate their liberation characteristics, and assess their association with gangue minerals.

Representative images obtained from the automated mineralogical analysis are presented in Figure 2. Gold particles were identified as discrete phases dispersed throughout the limonitic matrix and associated gangue

minerals. The observations allowed qualitative assessment of particle morphology, grain size, and degree of liberation, which are important parameters governing cyanidation performance.

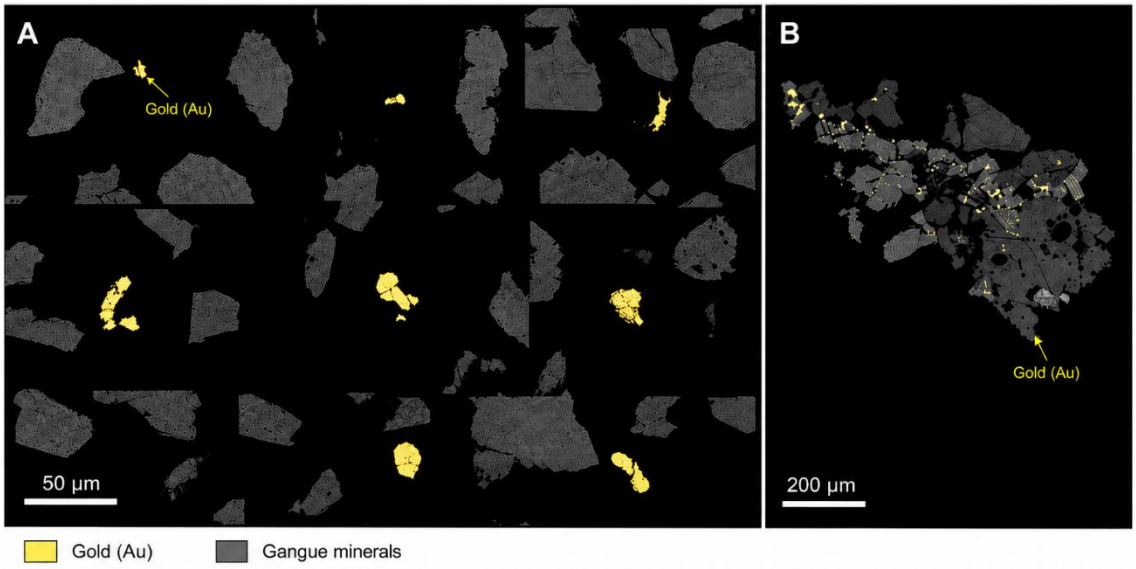

Figure 2. Automated mineralogical characterization of gold particles in the investigated limonitic ore samples. Gold particles identified by automated mineralogical analysis are highlighted and labeled as Au. (A) Representative high-magnification images illustrating the morphology and liberation characteristics of individual gold particles (scale bar = 50 µm). (B) Low-magnification overview showing the spatial distribution of gold particles within the sample (scale bar = 200 µm). Authors' own elaboration based on QEMSCAN and SEM-EDS analyses.

The automated mineralogical observations indicate that gold occurs predominantly as discrete particles distributed throughout the gangue matrix. Most particles appear to be liberated or only weakly associated with neighboring mineral phases, suggesting favorable exposure to the cyanide solution during leaching. Gold particle sizes range from a few to several tens of micrometers, indicating that a significant proportion of the gold is potentially accessible without ultrafine grinding.

The broader field of view shown in Figure 2(B) confirms the heterogeneous yet widespread distribution of gold across the investigated samples. These observations provide mineralogical support for the cyanidation behavior discussed in subsequent sections and contribute to the interpretation of gold extraction kinetics from leaching tests.

Dynamic Cyanidation Tests

Dynamic cyanidation tests were conducted to determine the maximum achievable gold extraction and the corresponding cyanide consumption under intensive leaching conditions.

Prior to cyanide addition, pulp pH was adjusted to 10.5 using hydrated lime to prevent hydrogen cyanide formation and to establish favorable conditions for gold dissolution. The pulp was maintained under agitation for at least 15 minutes before cyanide addition.

Leaching experiments were carried out in 4-L glass reactors equipped with mechanical agitation and air sparging. Sodium cyanide was used as the lixiviant at an initial concentration of 500 mg/L.

The main operating conditions were:

- Particle size: <75 µm;
- Solids concentration: 45 wt%;

- Initial NaCN concentration: 500 mg/L;
- pH: 10.3–10.5;
- Temperature: ambient;
- Leaching duration: 24 h.

At the end of each test, slurry samples were filtered, and both residues and pregnant solutions were analyzed to determine gold extraction and cyanide consumption.

Kinetic Cyanidation Tests

Kinetic cyanidation experiments were conducted using Samples 01–04 to evaluate the relationship between gold extraction, cyanide consumption, and leaching time under conditions representative of industrial operations.

Approximately 1 kg of ore with particle size below 6.35 mm was placed into 5-L leaching bottles. The pulp pH was adjusted to 10.5 using hydrated lime prior to cyanide addition. The operating conditions were identical to those employed in the dynamic cyanidation tests, except for particle size and total leaching duration.

Sampling intervals were established at 2, 4, 6, 8, 24, 48, 72, and 96 h. At each sampling interval, free cyanide concentration was measured and adjusted when necessary. Gold concentrations in solution were determined by atomic absorption spectrometry, allowing the calculation of cumulative gold extraction and cyanide consumption as a function of leaching time.

To validate the metallurgical response of the ore population, Samples 05–14 were subjected to standardized cyanidation tests using the same operating conditions adopted for the kinetic experiments. However, only the final gold extraction after 8 h of leaching was determined for these samples. Residual gold contents in the leach residues were measured by fire assay, allowing calculation of the corresponding extraction efficiencies.

Calculation of Gold Extraction

Gold extraction was calculated according to Equation (1):

$$\textbf{Gold Extraction (\%)} = (m_{Au,solution}/m_{Au,feed}) \times 100$$

where:

- $m_{Au,\ solution}$ is the mass of gold dissolved in solution;
- $m_{Au,\ feed}$ is the mass of gold initially present in the ore sample.

Statistical Analysis

Dynamic cyanidation tests were performed in triplicate, whereas kinetic leaching experiments were conducted in duplicate. Mean values and standard deviations were calculated for gold extraction and sodium cyanide consumption at each sampling interval.

The expanded dataset comprising fourteen samples was used to evaluate the variability of cyanidation performance within the investigated limonitic weathering domain. Descriptive statistical parameters, including mean, median, minimum, maximum, range, standard deviation, coefficient of variation, quartiles, and interquartile range, were calculated for gold extraction.

Linear regression analysis was applied to evaluate the relationships between sulfur content and gold extraction for Samples 05–14 and between copper content and sodium cyanide consumption for Samples 01–04. The coefficient of determination (R^2) was used to quantify the strength of the observed correlations.

Graphical statistical tools, including scatter plots and box plots, were employed to assess data distribution, identify trends, and detect potential outliers within the investigated sample population.

Because the additional validation samples (Samples 05–14) were represented by single cyanidation determinations, inferential statistical comparisons among these samples were not performed. Consequently, the statistical evaluation of the expanded dataset was restricted to descriptive statistics and correlation analyses, which were considered appropriate for assessing metallurgical variability within the investigated weathering domain.

Experimental Workflow

The overall experimental methodology consisted of:

1. Sample preparation and comminution;
2. Chemical characterization;
3. Mineralogical characterization (Samples 01–04);
4. Dynamic cyanidation testing (Samples 01–04);
5. Kinetic cyanidation testing (Samples 01–04);
6. Standardized 8 h cyanidation tests (Samples 05–14);
7. Determination of gold extraction;
8. Determination of cyanide consumption;
9. Statistical evaluation and validation of metallurgical performance.

RESULTS AND DISCUSSION

Chemical and Mineralogical Characteristics of the Ores

Mineralogical analyses showed variability among samples from the same weathering system. Iron oxyhydroxides dominated in SAMPLE 01, SAMPLE 03, and SAMPLE 04, making up 72-77 wt.%, while SAMPLE 02 had only 14 wt.% iron oxyhydroxides and a higher quartz and silicate content.

SAMPLE 01, 03, and 04 are typical limonitic laterites; SAMPLE 02 is a more silicate-rich horizon. Variability reflects differences in weathering, groundwater, and parent rock in tropical systems.

The predominance of iron oxyhydroxides confirms extensive supergene alteration and suggests that most sulfide minerals originally present in the deposit have been oxidized. This interpretation is further supported by the extremely low sulfur contents measured in all samples.

Gold grades ranged from 1.2 to 1.9 g/t, which are representative of low-grade disseminated gold deposits currently exploited by large-scale mining operations worldwide. Copper concentrations varied from 0.02 to 0.30 wt.%, while manganese contents ranged between 0.1 and 2.2 wt.%.

The chemical composition of the limonitic ores is shown in Table 1.

Table 1. Chemical composition of the investigated limonitic gold ores. Source: Generated in this study from ICP-OES, fire assay, and carbon analyses.

Sample	Au (g/t)	Cu (wt.%)	Fe (wt.%)	Mn (wt.%)	Si (wt.%)	Al (wt.%)	C (wt.%)	S (wt.%)
Sample 01	1.6	0.10	37.1	0.1	13.6	5.1	0.23	0.02
Sample 02	1.9	0.30	13.3	2.2	29.6	4.2	0.34	0.02
Sample 03	1.7	0.07	48.2	0.3	5.5	4.6	0.06	0.02
Sample 04	1.2	0.02	47.2	0.2	10.6	3.0	0.06	0.02

The chemical characterization reveals significant variability among the limonitic ores. Iron content varied considerably, indicating different levels of weathering and iron enrichment. Sulfur levels were low, showing extensive oxidation of sulfides and classifying the ores as mostly oxidized. Copper levels varied from trace to about 0.30 wt.%, hinting at differences in cyanide consumption during leaching.

Chemical analyses give valuable bulk composition data but don't reveal mineral forms. Automated mineralogical characterization via QEMSCAN quantified mineralogy and identified key mineral phases affecting gold extraction and reagent use, summarized in Table 2.

Table 2. Modal mineralogy of Samples 01–04 (wt.%). Source: Generated in this study from QEMSCAN analysis.

Mineral	Sample 01	Sample 02	Sample 03	Sample 04
Iron oxyhydroxides	76.8	14.2	71.8	63.2
Quartz	5.7	52.0	1.3	18.7
Chlorite	3.2	9.3	4.2	1.6
Biotite	0.0	0.1	5.2	1.0
Garnet	4.0	12.3	10.2	6.4
Kaolinite	9.3	3.3	5.1	8.0
Mn oxides	0.1	4.0	0.1	0.0
Others	0.9	4.9	2.1	1.1

The SEM-EDS observations demonstrated that manganese oxides frequently occur along fractures and discontinuities, whereas biotite and iron oxyhydroxides form complex mineral assemblages that may host secondary copper minerals. These textural relationships are important because they directly influence cyanide consumption and leaching performance.

Detailed SEM-BSE and EDS analyses were performed to investigate the textural relationships among iron oxyhydroxides, copper-bearing phases, manganese oxides, and silicate minerals. Particular attention was given to identifying phases potentially associated with cyanide consumption and to understanding the mineralogical controls on gold extraction. Representative micrographs and corresponding EDS spectra are presented in Figure 3.

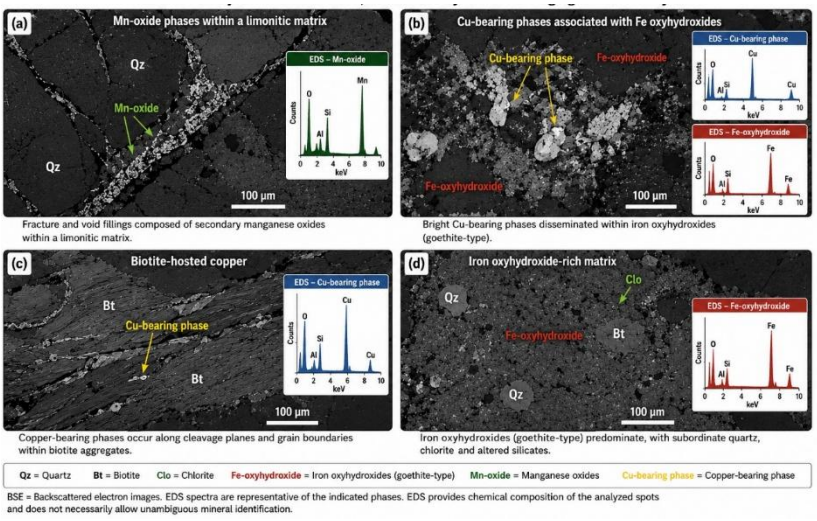

Figure 3. Representative SEM-BSE images and EDS spectra of the investigated limonitic ores. (a) Secondary manganese oxides filling fractures and voids within a limonitic matrix; (b) disseminated copper-bearing phases associated with iron oxyhydroxides; (c) copper-bearing phases occurring along

cleavage planes and grain boundaries within biotite aggregates; and (d) iron oxyhydroxide-rich matrix containing subordinate quartz, chlorite, and altered silicates. Abbreviations: Qz = quartz; Bt = biotite; Clo = chlorite. Source: This study.

The SEM-BSE observations reveal a complex weathering assemblage dominated by iron oxyhydroxides, with subordinate quartz, biotite, chlorite, and secondary manganese oxides. Manganese oxides commonly occur as fracture and pore fillings (Figure 3a), indicating precipitation during supergene alteration processes. Copper-bearing phases were observed both disseminated within iron oxyhydroxides (Figure 3b) and concentrated along cleavage planes and grain boundaries in biotite aggregates (Figure 3c), suggesting that copper was mobilized and redistributed during weathering. These mineralogical associations are particularly important because copper-bearing minerals are known to consume cyanide by forming stable copper–cyanide complexes, thereby increasing reagent demand during gold extraction (Pereira et al., 2017; Chen et al., 2020). The predominance of iron oxyhydroxides (Figure 3d) confirms the strongly oxidized nature of the deposit and is consistent with the low sulfur contents measured in all samples. Recent studies have shown that iron oxyhydroxides may host fine gold particles or act as adsorption sites for dissolved gold species, although their influence on gold recovery depends strongly on mineral texture and gold deportment (Huang et al., 2025; Roostaei et al., 2025).

The absence of significant sulfide mineralization indicates that the investigated ores should not be classified as refractory in the conventional sense. Instead, gold accessibility is expected to be controlled primarily by mineral liberation and by interactions with iron oxyhydroxides and secondary copper-bearing phases (Pereira et al., 2017).

The detailed mineralogical characterization was performed on Samples 01–04, which were selected as representative of the investigated limonitic weathering domain. The additional samples (Samples 05–14) originated from the same geological environment and exhibited similar field characteristics, weathering intensity, and lithological associations. Consequently, the mineralogical interpretation developed from Samples 01–04 was considered representative of the broader ore population evaluated in this study.

Dynamic Cyanidation Performance

Dynamic cyanidation tests were performed using finely ground material (<75 μm) to evaluate the maximum achievable gold extraction under intensive leaching conditions.

Gold extraction values ranged from approximately 85% to 94%, with an average recovery close to 89–90%. These recoveries indicate that most of the gold present in the investigated ores is readily accessible to cyanide dissolution.

According to modern classifications of gold ores, recoveries exceeding approximately 80–85% without oxidative pretreatment are generally indicative of free-milling behavior. Therefore, the investigated limonitic ores can be classified as free-milling ores despite their high iron content.

The high recoveries observed are likely attributable to the deposit's advanced oxidation state. During lateritization, sulfides are destroyed, and gold particles become progressively exposed, facilitating cyanide access. This mechanism contrasts sharply with that in refractory sulfide ores, where gold remains encapsulated within pyrite, arsenopyrite, or other sulfide minerals (Pereira et al., 2018).

Although extraction levels were relatively uniform among the samples, cyanide consumption exhibited greater variability. The average sodium cyanide consumption was approximately 946 g NaCN/t ROM, which is considered moderate to high for oxidized gold ores.

The discrepancy between relatively constant gold recovery and variable cyanide consumption suggests that cyanide-consuming minerals exert a stronger influence on reagent consumption than on gold dissolution.

The results of the dynamic cyanidation tests are presented in Table 3

Table 3. Dynamic cyanidation results for finely ground material (<75 µm). Source: Generated in this study

Sample	Head grade (g/t Au)	Residual Au (g/t)	Gold extraction (%)
Sample 01	1.6	0.24	85.0
Sample 02	1.9	0.22	88.4
Sample 03	1.7	0.17	90.0
Sample 04	1.2	0.07	94.2
Mean	—	—	89.4

The dynamic cyanidation tests demonstrated that the investigated limonitic ores are highly amenable to gold extraction under conventional cyanidation conditions. Gold recoveries ranged from 85.0% to 94.2%, with an average recovery of approximately 89.4%, despite the considerable mineralogical variability observed among the samples. These results indicate that most of the gold present is readily accessible to cyanide dissolution and that extensive refractory behavior is absent.

The relatively high recoveries observed in samples with high proportions of iron oxyhydroxides suggest that limonitic enrichment does not necessarily hinder gold extraction. In contrast, the observed differences in cyanide consumption among the samples suggest that factors other than gold accessibility may play a greater role in determining process economics. In particular, the variable concentrations of copper-bearing phases identified during mineralogical characterization suggest that copper may be an important cyanide-consuming component in the investigated ores.

These observations indicate that mineralogical composition exerts a stronger influence on reagent consumption than on gold recovery itself. To further evaluate this relationship, the influence of copper-bearing minerals on sodium cyanide consumption was investigated using the kinetic leaching data and chemical characterization results.

Influence of Copper on Cyanide Consumption

Copper was the main factor controlling cyanide use. SAMPLE 02, with the highest copper (0.30 wt.%), also showed the highest cyanide consumption in leaching tests. This aligns with copper minerals forming stable copper-cyanide complexes.

The relationship between copper content and cyanide consumption was further evaluated to identify the principal factors controlling reagent demand during cyanidation. Copper-bearing minerals were observed in association with iron oxyhydroxides and altered silicates (Figure 3), suggesting that copper dissolution could significantly contribute to cyanide consumption. To quantify this effect, sodium cyanide consumption measured after 8 h of leaching was correlated with each sample's copper content, as shown in **Error! Reference source not found.**.

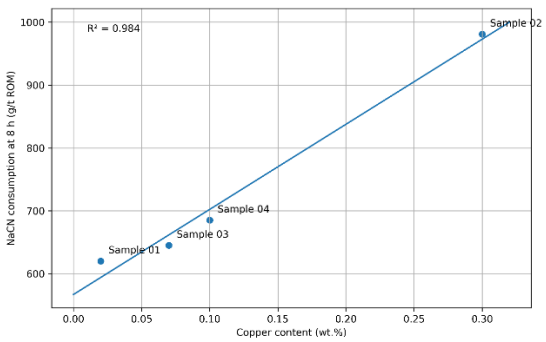

Figure 4. Relationship between copper content and sodium cyanide consumption after 8 h of cyanidation for the investigated limonitic ores. The linear regression ($R^2 = 0.984$) suggests a strong influence of copper-bearing phases on cyanide demand. Source: This study.

Figure 4 reveals a strong positive correlation between copper content and sodium cyanide consumption, with a coefficient of determination (R^2) of 0.984. The sample containing the highest copper concentration (0.30 wt.% Cu; Sample 02) exhibited the highest cyanide consumption, whereas samples with lower copper contents consumed substantially less reagent. This relationship indicates that copper-bearing minerals are important cyanide-consuming phases in the investigated ores. The dissolution of copper minerals forms stable copper–cyanide complexes, thereby reducing the concentration of free cyanide available for gold dissolution and consequently increasing reagent consumption (Pereira et al., 2017, 2018; Chen et al., 2020).

Mineralogical characterization could help estimate cyanide demand and optimize processes during metallurgical evaluation. However, limited samples prevent firm conclusions. The trend aligns with copper minerals' known influence on cyanide use, as copper dissolution forms complexes that consume cyanide, reducing its availability for gold. Removing copper minerals before cyanidation can cut reagent costs—methods include acid leaching, ammonia, glycine, or flotation. Since cyanide costs impact overall operations, lowering reagent use without harming gold recovery can boost project economics.

Effect of Iron Oxyhydroxides on Gold Extraction

One of the most significant findings of this study is that high concentrations of iron oxyhydroxides did not adversely affect gold extraction.

Samples with over 70 wt.% iron oxyhydroxides had gold recoveries similar to those of silicate-rich samples, indicating that iron oxyhydroxides didn't significantly encapsulate gold or hinder cyanide access.

Automated mineralogical observations indicate that a substantial proportion of the gold occurs as liberated or weakly associated particles, which is consistent with the high cyanidation recoveries achieved.

Nevertheless, iron oxyhydroxides may still indirectly influence cyanidation. Goethite and ferrihydrite have high surface areas and can adsorb dissolved metals. In industry, such adsorption may affect solution chemistry and carbon adsorption during recovery.

Further investigation using automated mineralogy and gold deportment analyses would be valuable for quantifying the exact distribution of gold among the various mineral phases.

Cyanidation Kinetics

The kinetic leaching experiments demonstrated rapid gold dissolution during the first hours of cyanidation.

Table 4. Gold extraction as a function of cyanidation time. Source: Generated in this study.

Time (h)	Sample 01	Sample 02	Sample 03	Sample 04	Mean
2	69.0	41.6	55.6	69.7	59.0
4	77.1	66.6	76.9	69.8	72.6
6	87.6	84.5	89.5	78.9	85.1
8	89.6	91.2	91.5	89.9	90.5
24	89.6	91.2	91.8	91.2	91.0
48	96.2	95.1	91.8	92.7	94.0
72	97.3	95.1	94.3	96.2	95.7
96	97.3	95.9	94.3	96.2	95.9

Average gold extraction increased from approximately 59% after 2 h to approximately 90% after only 8 h of leaching. Thereafter, the extraction rate decreased substantially, and only limited additional recovery was observed despite extending the leaching time to 96 h.

To evaluate the leaching behavior of the limonitic ores, gold extraction was Figure 5 shows extraction profiles for four samples monitored over the cyanidation period. Despite differences in mineralogy and copper, all samples rapidly dissolved gold initially, then more slowly as equilibrium was reached. The average curve and standard deviation indicate reproducibility and help determine optimal residence time.

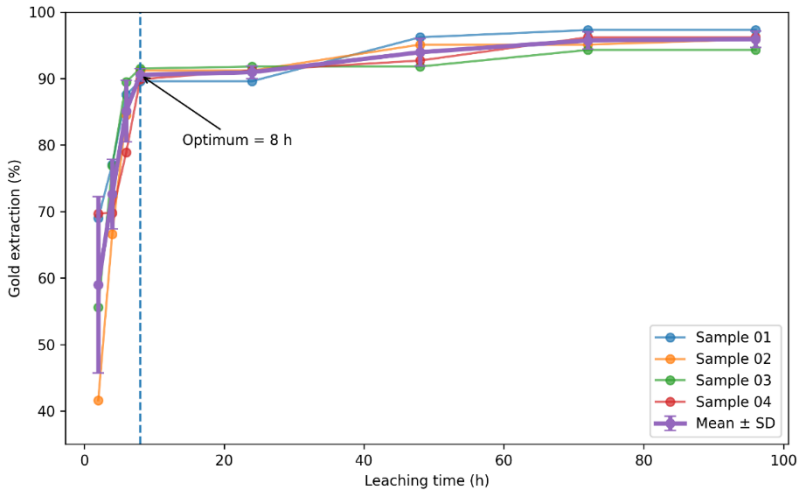

Figure 5. Gold extraction as a function of leaching time for the four limonitic ore samples investigated. Error bars represent ±1 standard deviation based on the average recovery of all samples. The dashed vertical line indicates the optimum leaching time of 8 h, at which approximately 90.5% average gold recovery was achieved. Source: This study.

As shown in Figure 5, gold dissolution occurred rapidly during the first hours of cyanidation, with average recovery increasing from 59.0% after 2 h to 90.5% after 8 h. Thereafter, the extraction rate decreased markedly, and only marginal improvements were observed despite extending the leaching period to 96 h. The results indicate that most of the readily accessible gold was dissolved within the first 8 h of leaching, confirming the favorable kinetics and free-milling nature of the investigated limonitic ores. Consequently, longer residence times primarily increased reagent consumption rather than significantly improving gold recovery.

This behavior is characteristic of free-milling ores and suggests that most accessible gold dissolves rapidly once cyanide and oxygen are available.

From an industrial perspective, the results indicate that prolonged leaching beyond 8 h may not be economically justified. While extraction increased slightly between 8 h and 96 h, cyanide consumption increased dramatically over the same period.

The average cyanide consumption increased from approximately 649 g NaCN/t ROM at 8 h to nearly 1,600 g NaCN/t ROM after 96 h. Consequently, the additional gold recovered at longer residence times is unlikely to compensate for the substantially higher reagent costs.

Although gold extraction provides the primary measure of metallurgical performance, reagent consumption is often one of the most important economic parameters in cyanidation circuits. Consequently, sodium cyanide consumption was monitored throughout the kinetic leaching experiments to evaluate the relationships among leaching time, reagent demand, and gold recovery. Particular attention was given to identifying the operating condition that maximizes metallurgical performance while minimizing cyanide consumption. The sodium cyanide consumption data obtained for Samples 01–04 are summarized in Table 5.

Table 5. Sodium cyanide consumption as a function of cyanidation time. Source: Generated in this study.

Time (h)	Sample 01	Sample 02	Sample 03	Sample 04	Mean
2	362	820	440	389	503
4	381	832	501	412	532
6	495	932	476	512	604
8	605	981	499	511	649
24	930	1180	831	843	946
48	990	1482	1478	1161	1278
72	1139	1692	1502	1391	1431
96	1309	2011	1506	1530	1589

Gold extraction plateaued after about 8 hours of cyanidation, but sodium cyanide use kept increasing. This shows that longer times improve gold recovery little but raise reagent costs. Therefore, monitoring cyanide demand over time is crucial to find the most cost-effective conditions.

Because the cyanidation experiments were conducted using four mineralogically distinct ore samples, a statistical evaluation was performed to assess whether the observed differences in gold recovery at the optimum leaching time were significant. Replicated cyanidation results obtained for Samples 01–04 at the optimum cyanidation time (8 h) were compared, and the results are summarized in Table 6.

Statistical analysis checked if gold recovery differences among samples exceeded variability and heterogeneity. Probabilities over 0.05 were not significant, indicating similar cyanidation. Values below 0.05 revealed mineralogy and chemistry significantly impacted gold extraction, supporting metallurgical results and cyanidation conclusions.

Figure 6 presents the sodium cyanide consumption profiles for Samples 01–04 together with the mean values and standard deviations calculated from the experimental dataset.

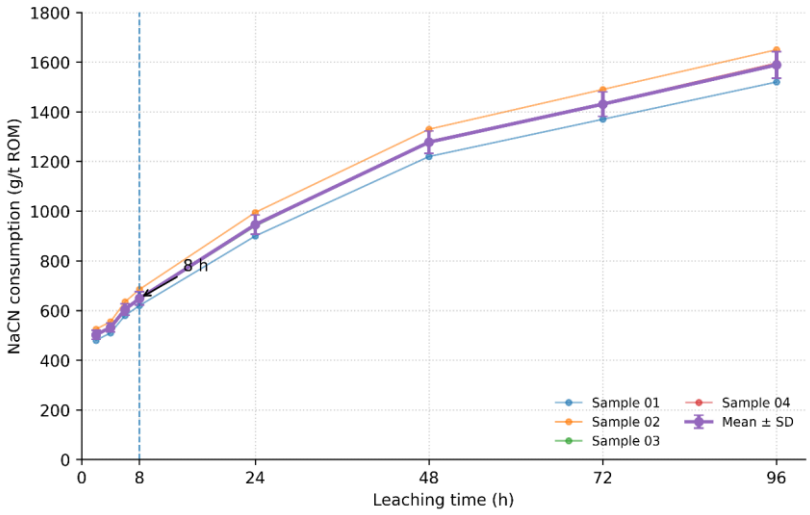

Figure 6. Sodium cyanide consumption as a function of cyanidation time for Samples 01–04. The dashed vertical line indicates the optimum leaching time of 8 h, corresponding to the most favorable balance between gold recovery and reagent consumption. Error bars represent ± one standard deviation. Source: Generated in this study.

Figure 6 shows that sodium cyanide consumption increased continuously during the entire leaching period, even after gold extraction had approached its maximum values. The average cyanide consumption increased from approximately 649 g NaCN/t ROM at 8 h to nearly 1,600 g NaCN/t ROM after 96 h, representing an increase of approximately 145% while gold recovery improved by only about 5 percentage points. This behavior demonstrates that extending the leaching period beyond 8 h results in diminishing metallurgical returns and substantially higher reagent costs.

Notable differences in cyanide use were seen across samples. Sample 02 had the highest sodium cyanide demand at about 1,650 g NaCN/t ROM after 96 hours, while Sample 01 had the lowest. These variations align with copper content data and suggest copper minerals mainly drive cyanide consumption in the ores.

Analysis of Figures 5 and 6 shows an optimal cyanidation time of about 8 hours, balancing gold recovery and reagent use. At this point, average gold recovery was 90.5%, with sodium cyanide consumption under 650 g NaCN/t ROM. Longer times are unlikely to be economically justified.

These findings demonstrate that optimizing residence time is an effective strategy for minimizing operating costs while maintaining high gold recovery.

The 8-hour leaching time from the kinetic experiments was used as the reference for testing 10 additional limonitic ore samples from the same area. This larger dataset was used to evaluate cyanidation variability and validate the study's conclusions.

Validation of Cyanidation Performance Using Additional Samples

To assess the representativeness of the metallurgical behavior of Samples 01–04, 10 additional limonitic ore samples from the same weathering domain underwent 8 h cyanidation tests, as per the kinetic study. These samples were used to evaluate gold extraction variability and to validate previous mineralogical and kinetic conclusions. Table 6 shows gold grades, sulfur contents, residual gold, and extraction efficiencies for Samples 05–14.

Table 6. Gold grades, sulfur contents, residual gold after cyanidation, and extraction efficiencies for Samples 05–14 after 8 h of cyanidation. Source: This study.

Sample	Au Grade (g/t)	Sulfur (%)	Residual Au After Cyanidation (g/t)	Gold Extraction (%)
Sample 05	2.330	<0.010	0.0600	97.5
Sample 06	26.533	<0.010	0.0967	99.6
Sample 07	20.350	<0.010	0.1933	99.1
Sample 08	0.557	0.011	0.0867	83.2
Sample 09	2.283	<0.010	0.0900	96.0
Sample 10	2.777	<0.010	0.1567	94.4
Sample 11	0.973	0.035	0.0567	94.3
Sample 12	1.107	0.284	0.5033	55.0
Sample 13	2.970	<0.010	0.0600	98.0
Sample 14	2.233	0.013	0.0433	98.0

The results presented in Table 6 demonstrate the generally favorable cyanidation behavior of the investigated limonitic ores. Gold recoveries ranged from 55.0% to 99.6%, with an average value of 91.5%. Most samples achieved recoveries above 90%, confirming the predominantly free-milling character of the ore population. Sample 12 exhibited markedly lower extraction (55.0%) and had the highest sulfur concentration (0.284 wt.%

S), suggesting the presence of residual sulfide mineralization that can reduce cyanidation efficiency. In contrast, samples containing sulfur contents below approximately 0.05 wt.% consistently achieved high gold recoveries, indicating that advanced oxidation of the weathering profile generally favors gold accessibility to cyanide solutions.

Gold recoveries ranged from 55.0% to 99.6%, with an overall average recovery of 91.5%. Nine of the ten samples achieved recoveries exceeding 83%, while seven samples exhibited recoveries greater than 94%. These results confirm the generally favorable cyanidation behavior of the investigated limonitic ores.

The lowest recovery (55.0%) was observed for Sample 12, which also contained the highest sulfur concentration (0.284 wt.% S). In contrast, samples containing sulfur concentrations below approximately 0.05 wt.% consistently achieved recoveries above 90%. This behavior suggests that residual sulfide mineralization may locally reduce cyanidation performance despite the predominantly oxidized nature of the deposit.

The expanded dataset provides independent validation of the free-milling characteristics identified in the detailed mineralogical and kinetic investigation. Although localized variations occur within the weathering profile, the overall metallurgical response demonstrates that the investigated limonitic ores are highly amenable to conventional cyanidation.

Statistical Assessment of Gold Recovery and Sulfur Content

The inclusion of ten additional samples enabled a broader statistical evaluation of cyanidation performance within the investigated limonitic weathering domain. Gold recovery exhibited a mean value of 91.5%, a median of 96.8%, and a standard deviation of 13.5%. The relatively large dispersion was primarily attributable to Sample 12, which behaved anomalously as a sulfur-rich sample.

When Sample 12 was excluded from the analysis, the average gold recovery increased to 95.6%, while the standard deviation decreased to 4.8%. This result demonstrates that the majority of the investigated ore population exhibits highly consistent cyanidation behavior characteristic of free-milling oxidized gold ores.

A strong inverse relationship exists between sulfur content and gold recovery, with a linear regression showing $R^2 \approx 0.90$. This indicates sulfur as a key predictor of cyanidation performance. Even low residual sulfides may hinder gold extraction. To investigate factors affecting cyanidation, the relationship between sulfur content and gold extraction was examined using additional samples (05–14). Sulfur was considered a potential indicator of residual sulfides, as mineralogical analysis showed the ores are mostly oxidized with minor sulfur. However, localized sulfides may remain in the weathering profile, affecting gold accessibility during cyanidation. This relationship is shown in Figure 7.

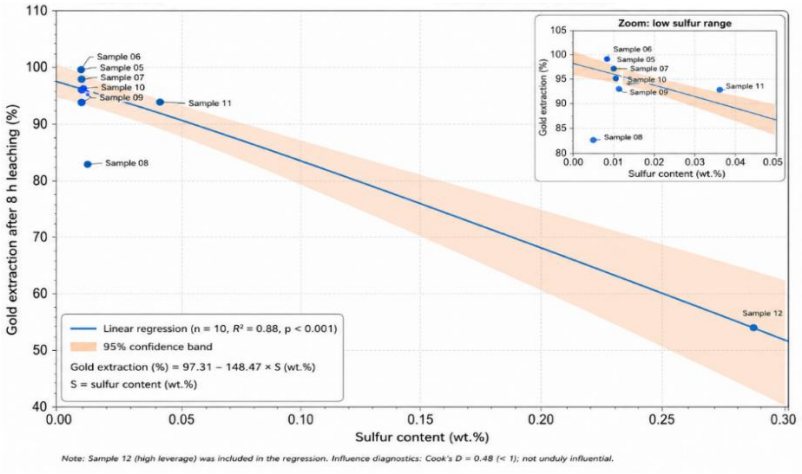

Figure 7. Relationship between sulfur content and gold extraction for Samples 05–14 after 8 h of cyanidation. The regression line indicates a strong inverse correlation between sulfur concentration and gold recovery.

As shown in Figure 7, a strong inverse correlation exists between sulfur concentration and gold extraction, indicating that residual sulfide mineralization may significantly affect cyanidation performance despite the deposit's overall oxidized nature. The sample containing the highest sulfur content exhibited the lowest gold recovery, supporting the interpretation that sulfur-bearing phases represent the principal source of metallurgical variability within the investigated ore population.

Sulfur content is interpreted only as an indirect indicator of residual sulfide occurrence because detailed mineralogical identification of sulfides was not performed for Samples 05–14

To complement the correlation analysis, the distribution of gold recovery values was evaluated using descriptive statistical methods. Box plots provide a concise visualization of data dispersion, central tendency, and potential outliers, allowing a more comprehensive assessment of metallurgical variability within the ore population. Figure 8 presents the distribution of gold recovery values obtained for Samples 05–14 after 8 h of cyanidation and highlights the overall consistency of cyanidation performance among the investigated limonitic ores.

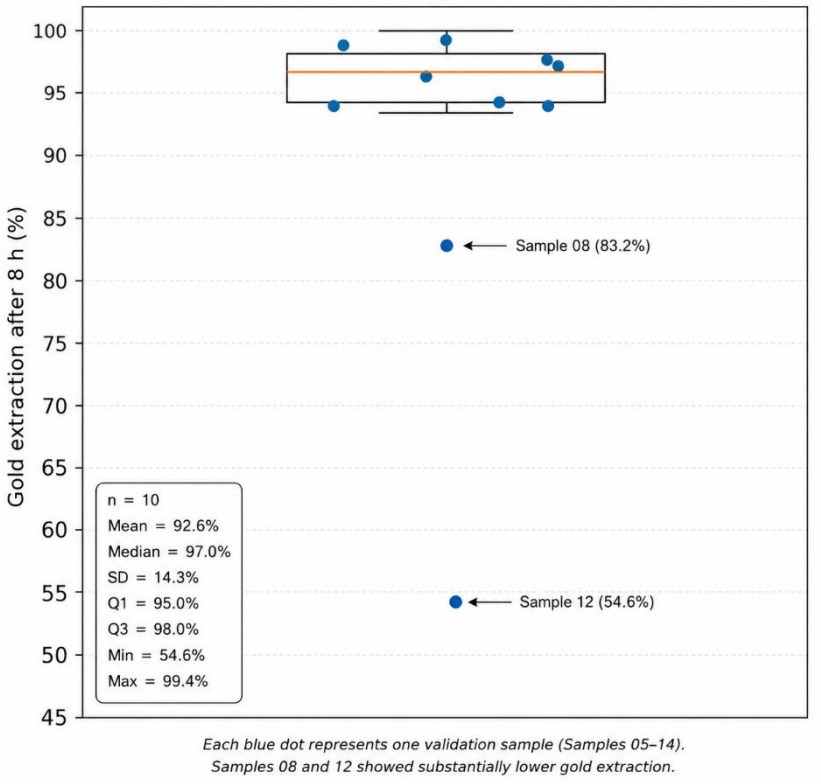

Figure 8. Box plot showing the distribution of gold recovery values for Samples 05–14 after 8 h of cyanidation.

Figure 8 shows that most samples fall within a relatively narrow recovery interval above 90%, confirming the predominantly free-milling nature of the investigated limonitic ores. The median recovery is approximately 96.8%, and the interquartile range is comparatively small, indicating limited variability across most samples. A single outlier, corresponding to Sample 12, exhibits substantially lower recovery and reflects the influence of residual sulfur-bearing phases identified through the sulfur content analysis. The distribution therefore supports the conclusion that the investigated ore population is highly amenable to cyanidation, with localized sulfide-rich zones representing the principal source of metallurgical variability.

To provide a quantitative overview of the cyanidation performance of the investigated ore population, descriptive statistics were calculated from the complete dataset comprising Samples 01–14. The resulting statistics (Table 7) summarize the central tendency, dispersion, and overall variability of gold extraction within the limonitic weathering domain and provide additional support for classifying these ores as predominantly free-milling.

Table 7.. Statistical summary of the 14-sample population

Parameter	Value
n	14
Mean	90.8
Median	94.4
SD	12.6
CV (%)	13.9
Min	55.0
Max	99.6
CI95	xx–xx

The descriptive statistics confirm the favorable cyanidation behavior of the investigated limonitic ores. The mean gold recovery exceeded 90%, while the median recovery of 94.4% indicates that most samples achieved high extraction efficiencies. Although the coefficient of variation reached approximately 14%, reflecting natural geological variability within the weathering profile, the majority of samples exhibited recoveries above 90%. The lower recovery observed for one sample (55.0%) is the principal source of variability and is attributed to localized mineralogical heterogeneity and residual sulfide. Overall, the statistical results support classifying the investigated ore population as predominantly free-milling and amenable to conventional cyanidation.

The statistical analysis therefore supports the mineralogical interpretation that the investigated ores are predominantly oxidized and free-milling, while also highlighting localized zones of residual sulfide mineralization that can degrade metallurgical performance. These findings emphasize the importance of integrating mineralogical characterization with metallurgical testing when evaluating the economic potential of limonitic gold deposits.

Although the individual cyanidation results presented in Table 6 demonstrate the generally favorable metallurgical response of the investigated limonitic ores, a broader statistical evaluation is required to quantify the variability of gold recovery within the ore population. Descriptive statistical parameters provide a useful framework for assessing the consistency of cyanidation performance and identifying anomalous samples that may reflect localized mineralogical variations. Table 8 summarizes the principal statistical indicators calculated for the gold extraction data obtained from Samples 05–14 after 8 h of cyanidation.

Table 8. Descriptive statistics of gold extraction for the investigated limonitic ore population (Samples 05–14) after 8 h of cyanidation.

Parameter	Gold Extraction (%)
Number of samples (n)	10
Mean	91.5
Median	96.8
Minimum	55.0
Maximum	99.6
Range	44.6
Standard deviation (SD)	13.5
Variance	181.1
Coefficient of variation (CV, %)	14.7

First quartile (Q1)	91.6
Third quartile (Q3)	98.0
Interquartile range (IQR)	6.4

The descriptive statistics confirm the high amenability of the ore population to cyanidation. Excluding the sulfur-rich outlier, the average gold recovery exceeded 95%, demonstrating the consistency of metallurgical performance within the investigated limonitic weathering domain.

Implications for Industrial Gold Processing

The metallurgical behavior observed in this study indicates that the investigated limonitic ores are highly amenable to conventional cyanidation processing. The detailed mineralogical characterization, dynamic cyanidation tests, kinetic leaching experiments, and validation conducted using an additional set of ten samples consistently demonstrated favorable gold extraction performance across the investigated weathering domain.

The dynamic cyanidation tests performed on finely ground material achieved average gold recoveries of approximately 89–90%, while the kinetic experiments showed that nearly 90% of the final recovery was attained within only 8 h of leaching. Furthermore, the expanded dataset comprising fourteen samples confirmed the predominance of free-milling behavior, with most samples exhibiting gold recoveries above 90%. These results indicate that conventional agitated-tank cyanidation represents a technically viable processing route for the investigated ores.

One of the most significant findings of this study is that high concentrations of iron oxyhydroxides did not adversely affect gold extraction. Samples containing more than 70 wt.% iron oxyhydroxides achieved recoveries comparable to those obtained for more silicate-rich material, demonstrating that gold accessibility was not significantly limited by the limonitic matrix. Instead, mineralogical composition exerted a stronger influence on cyanide consumption than on gold recovery.

Copper-bearing minerals were identified as the principal cyanide-consuming phases. The strong correlation observed between copper content and sodium cyanide consumption suggests that reagent demand can be predicted from mineralogical and chemical characterization. Consequently, future process optimization should focus on strategies to reduce cyanide consumption, including selective copper removal, targeted blending of high-copper ores, or alternative reagent schemes.

The statistical evaluation of the additional validation samples demonstrated that sulfur content is an important indicator of metallurgical variability within the weathering profile. While the majority of samples exhibited recoveries characteristic of free-milling oxidized ores, localized sulfur-rich zones produced significantly lower gold extraction. Therefore, sulfur content may represent a practical geometallurgical parameter for identifying potentially problematic ore domains and supporting mine planning decisions.

Overall, the results demonstrate the importance of integrating mineralogical characterization, metallurgical testing, and statistical validation during process development and feasibility studies. Such an approach improves the prediction of gold recovery and reagent consumption, reduces technical uncertainty, and provides a more robust basis for the design and optimization of gold-processing operations involving limonitic and lateritic ores.

CONCLUSIONS

The cyanidation behavior of gold-bearing limonitic ores from the Carajás Mineral Province was investigated through integrated chemical, mineralogical, and metallurgical characterization combined with dynamic and kinetic leaching experiments. Four representative samples were subjected to detailed mineralogical analysis, while an additional ten samples were evaluated through standardized cyanidation tests to validate the metallurgical response of the ore population.

The investigated ores are characterized by advanced weathering, high proportions of iron oxyhydroxides, and low sulfur contents, confirming their predominantly oxidized nature. Despite significant mineralogical variability among the samples, cyanidation performance remained consistently high.

Dynamic cyanidation tests performed on material ground to below 75 μm achieved average gold recoveries of approximately 89–90%, indicating that most of the gold is readily accessible to cyanide dissolution. Samples containing up to 77 wt.% iron oxyhydroxides exhibited gold recoveries comparable to those obtained for more silicate-rich materials, suggesting that the abundance of limonitic phases does not constitute a major limitation to gold extraction under the investigated conditions.

Gold dissolution occurred rapidly during the initial stages of leaching, with approximately 90% of the final recovery achieved after only 8 h of cyanidation. Extending the leaching time beyond this period resulted in only marginal increases in gold recovery while substantially increasing sodium cyanide consumption. Consequently, 8 h was identified as the optimum cyanidation time, yielding an average gold recovery of 90.5% with a sodium cyanide consumption of approximately 650 g NaCN/t ROM.

Copper-bearing minerals were identified as the principal contributors to cyanide consumption. An increasing trend between copper content and sodium cyanide demand was observed, indicating that copper mineralization represents an important factor controlling reagent consumption and should be considered during process design and geometallurgical evaluation.

The expanded dataset comprising fourteen samples confirmed the predominantly free-milling character of the investigated ores, with most samples achieving gold recoveries above 90%. The only sample exhibiting substantially lower recovery was characterized by elevated sulfur content, suggesting that localized remnants of sulfide mineralization may negatively influence cyanidation performance even within an overall oxidized weathering profile.

Overall, the results demonstrate that the investigated limonitic ores are suitable candidates for conventional cyanidation processing and can be classified predominantly as free-milling oxidized gold ores. The integration of mineralogical characterization, cyanidation kinetics, and metallurgical testing provided a robust framework for identifying the factors controlling gold recovery and reagent consumption, generating valuable information for geometallurgical characterization, process development, and economic evaluation of oxidized gold deposits.

Declarations

Funding

This research received no external funding.

Conflicts of Interest

The authors declare no conflict of interest.

Data Availability Statement

The data supporting the findings of this study are available from the corresponding author upon reasonable request.

Supplementary Materials

No supplementary materials are associated with this article.

Author Contributions: Antonio Clareti Pereira conceived the study, performed the investigation, analyzed the data, and wrote the manuscript. The author has read and approved the final version of the manuscript.

REFERENCES

1. Asamoah, R. K., Zanin, M., Addai-Mensah, J., & Skinner, W. (2021). Refractory gold ores and concentrates Part 1: Mineralogical and physico-chemical characteristics. *Mineral Processing and Extractive Metallurgy, 128*(4), 173–195. https://doi.org/10.1080/25726641.2019.1626659.
2. Bracamontes-Landavazo, M. A., Valenzuela-García, J. L., Parga-Torres, J. R., & Guerrero-German, P. (2024). Kinetic study for the extraction of gold and silver from an ore comparing lixiviants sodium cyanide and DEZO using moderate pressures. *Mining, Metallurgy & Exploration, 41*(5), 2589–2602. https://doi.org/10.1007/s42461-024-01036-9.
3. Bragin, V. I., Makarov, V. A., Usmanova, N. F., Samorodskii, P. N., Lobastov, B. M., & Vashlaev, A. I. (2019). Mineralogical examination of gold processing plant tailings. *Journal of Mining Science, 55*(1), 149–156. https://doi.org/10.1134/S1062739119015407.
4. Chen, G., Zhao, H., Zhou, J., Liu, Z., & Yang, H. (2025). Process mineralogy study and flotation testwork of a complex lead–gold rougher concentrate. *Minerals, 15*(9), 967. https://doi.org/10.3390/min15090967.
5. Chen, J., Zhong, S., Tang, D., & Kuang, C. (2020). Practical experience in large-scale development of Zijinshan low-grade gold-copper mine. *Mining, Metallurgy & Exploration, 37*(4), 1339–1347. https://doi.org/10.1007/s42461-020-00237-2
6. Chen, Z., Li, P., Wang, Q., & Dai, S. (2024). Study on adsorption of kaolinite and gold thiosulfate. *Scientific Reports, 14*, 15486. https://doi.org/10.1038/s41598-024-66389-z.
7. Chingwaru, S. J., Tadie, M., & von der Heyden, B. (2025). Characterization of gold in complex historical refractory tailings for enhanced process optimization. *Mineral Processing and Extractive Metallurgy Review, 46*(2), 193–209. https://doi.org/10.1080/08827508.2023.2298728.
8. Chingwaru, S.J., Von der Heyden, B. & Tadie, M. An underexploited invisible gold resource in the Archean sulphides of the Witwatersrand tailings dumps. *Sci Rep* **13**, 3086 (2023). https://doi.org/10.1038/s41598-023-30219-5.
9. Costa, F. R., Nery, G. P., Carneiro, C. C., Kahn, H., & Ulsen, C. (2022). Mineral characterization of low-grade gold ore to support geometallurgy. *Journal of Materials Research and Technology, 21*, 4303–4317. https://doi.org/10.1016/j.jmrt.2022.10.085.
10. Deveci, H., Yazıcı, E. Y., Celep, O., & Mercimek, M. (2022). Effects of lead nitrate and pre-aeration on the deportment of base/precious metals in cyanide leaching of a pyritic refractory gold concentrate. In *Proceedings of the 17th International Mineral Processing Symposium (IMPS 2022)*. Istanbul, Türkiye.
11. Grangeiro, L. C., Bevilaqua, D., Oliveira, K. B., Palmieri, M. C., & Macêdo, E. N. (2017). Avaliação do potencial biotecnológico para o tratamento de um minério de ouro de uma mina do estado do Amapá. *Tecnologia em Metalurgia, Materiais e Mineração, 14*(2), 107–118. https://doi.org/10.4322/2176-1523.1079.
12. Guner, M. K., Bulut, G., Hassanzadeh, A., Lode, S., & Aasly, K. (2023). Automated mineralogy and diagnostic leaching studies on bulk sulfide flotation concentrate of a refractory gold ore. *Minerals, 13*(10), 1243. https://doi.org/10.3390/min13101243.
13. Huang, F.-X., Wu, Y.-F., Evans, K., Williams-Jones, A. E., Zhao, X.-F., Wei, Y., Feng, W., & Li, J.-W. (2025). Adsorption and coarsening of gold nanoparticles in iron (oxyhydr)oxides lead to high-grade gold mineralization. *Geochimica et Cosmochimica Acta, 404*, 1–12. https://doi.org/10.1016/j.gca.2025.07.013.
14. Jia, Y., Wang, X., Cheng, W., & Ma, S. (2019). Research progress on non-cyanide leaching of refractory gold ores. *Chinese Journal of Engineering, 41*(3), 307–315. https://doi.org/10.13374/j.issn2095-9389.2019.03.003.
15. Lee, S., Sadri, F., & Ghahreman, A. (2024). Exploring non-ammoniacal thiosulfate gold leaching and limited gold recovery from a refractory gold ore oxidized in alkaline pressure conditions. *Journal of Sustainable Metallurgy, 10*(2), 486–496. https://doi.org/10.1007/s40831-024-00807-4.
16. Liu, X., Wang, Y., Han, P., Yan, J., & Ye, S. (2021). Leaching of gold from micro-disseminated oxidized gold ore by thiosulfate method. *Mining and Metallurgy, 30*(3). https://doi.org/10.3969/j.issn.1005-7854.2021.03.017.

17. Liu, X., Wang, Y., Xiao, L., Ma, L., Han, P., & Ye, S. (2022). Eco-friendly and rapid extraction of gold by in-situ catalytic oxidation with N-bromosuccinimide. *Heliyon, 8*(6), e09706. https://doi.org/10.1016/j.heliyon.2022.e09706.
18. Nicol, M. J. (2022). *Hydrometallurgy: Theory* (1st ed.). Elsevier. https://doi.org/10.1016/C2020-0-03551-.
19. Ofori-Sarpong, G., Adam, A.-S., Asamoah, R. K., & Amankwah, R. K. (2020). Characterisation of biooxidation feed and products for improved understanding of biooxidation and gold extraction performance. *International Journal of Mineral Processing and Extractive Metallurgy, 5*(2), 20–29. https://doi.org/10.11648/j.ijmpem.20200502.11.
20. Pereira, A. C., Barbosa, V. da S. B., & Rodrigues, M. L. M. (2017). Effectiveness of acidic pre-cleaning for copper-gold ore. REM - International Engineering Journal, 70(4), 445–450. DOI: 10.1590/0370-44672016700126
21. Pereira, A. C., Gomes, M. R. dos S., & Manfridini, A. P. D. A. (2018). Ensaios exploratórios de lixiviação para ouro associado a minérios limoníticos / Exploratory tests for leaching gold associated with limonitic ore. *Brazilian Applied Science Review, 3*(2). https://doi.org/10.34115/basr.v3i2.998
22. Qin, X., Hu, X., Li, J., Fu, Y., Wang, Q., Chen, Y., Wang, C., & coauthors. (2021). Effect of lead ions on gold dissolution in the Cu^{2+}–en–$S_2O_3^{2-}$ system. *Hydrometallurgy, 196*, 105430. https://doi.org/10.1016/j.hydromet.2020.105430.
23. Roostaei, H., Kordparijaei, M., & Mesroghli, S. (2025). Gold-bearing iron oxides processing based on ore characterization: Gravity pre-concentration and cyanide dissolution. *Journal of Sustainable Metallurgy, 11*(3), 3156–3168. https://doi.org/10.1007/s40831-025-01195-z.
24. Roostaei, H., Kordparijaei, M., & Mesroghli, S. (2026). Cyanide dissolution of gold-bearing iron oxide minerals: Kinetic studies and optimization using response surface methodology. *Discover Applied Sciences, 8*, 388. https://doi.org/10.1007/s42452-026-08420-8.
25. Sekisov, A., & Rasskazova, A. (2021). Assessment of the possibility of hydrometallurgical processing of low-grade ores in the oxidation zone of the Malmyzh Cu-Au porphyry deposit. *Minerals, 11*(1), 69. https://doi.org/10.3390/min11010069
26. Sevgül, S., Oluklulu, S., & Bozkurt, V. (2022). Concentration of an oxidized gold ore by the Knelson concentrator. In *Proceedings of the 17th International Mineral Processing Symposium (IMPS 2022)* (pp. 225–231). Istanbul, Türkiye.
27. Sitando, O., Senanayake, G., Dai, X., & Breuer, P. (2019). The adsorption of gold(I) on minerals and activated carbon (preg-robbing) in non-ammoniacal thiosulfate solutions: Effect of calcium thiosulfate, silver(I), copper(I), and polythionate ions. *Hydrometallurgy, 183*, 206–217. https://doi.org/10.1016/j.hydromet.2018.10.016
28. Soleymani Naeini, M. (2022). *Electrochemical study of gold thiosulfate extraction process* (Doctoral dissertation, Queen's University). Queen's University Research Repository. http://hdl.handle.net/1974/30384
29. Stephen, R. S., Anuar, W. N. S., Ismail, S., & Jabit, N. A. (2021). Characterisation and diagnostic leaching of gold-bearing mineral ore, East Coast Peninsular Malaysia. Malaysian Journal of Microscopy, 17(2). https://malaysianjournalofmicroscopy.org/ojs/index.php/mjm/article/view/535
30. Weng, Q., Zhan, W., Zhang, X., Song, S., Zeng, Z., Lwin, H. M., Arauz-Lara, J. L., & Jia, F. (2025). Electrochemical reduction and recovery of trace gold(I) from environmentally friendly thiosulfate leaching solutions using carbon electrodes. *Carbon, 232*, 119799. https://doi.org/10.1016/j.carbon.2024.119799
31. Yanbo, C., Qin, G., Li, G., & Zhu, X. (2021). Experimental study on thiosulfate leaching of gold from a high copper gold concentrate. *E3S Web of Conferences, 271*, 04001. https://doi.org/10.1051/e3sconf/202127104001.